ChemComm

Metal-Assisted Selective Recognition of Biothiols by a Synthetic Receptor Array

Journal:	*ChemComm*
Manuscript ID	CC-COM-09-2018-007220.R1
Article Type:	Communication

Journal Name

COMMUNICATION

Metal-Assisted Selective Recognition of Biothiols by a Synthetic Receptor Array

Received 00th January 20xx,
Accepted 00th January 20xx

DOI: 10.1039/x0xx00000x

www.rsc.org/

Yang Liu,[b] Yaokai Duan,[a] Adam D. Gill,[c] Lizeth Perez,[a] Qiaoshi Jiang,[b] Richard J. Hooley[a,c]* and Wenwan Zhong[a,b]*

A synergistic combination of a deep cavitand host, fluorophore guests and transition metal ions can be used to sense small molecule thiols of biological interest with good efficiency and selectivity in complex aqueous media.

Low-molecular-weight (LMW) thiols such as cysteine (**Cys**), homocysteine (**Hcy**) and glutathione (**GSH**) play crucial roles in biological systems as antioxidants and signaling agents, in metal sequestration and in protein biosynthesis.[1] The concentration, ratio and redox balance of these biothiols are controlled by diverse cellular processes, and disruption of this balance affects cell signaling and anti-pathogen response.[2] This has led to a need for simple survey techniques that allow monitoring of biothiol fluctuation and interplay in biological systems. Most probes for biothiols are reactivity-based, and exploit the innate nucleophilicity of thiol groups in conjugate addition reactions and fluorophore displacements for optical detection.[3] These are most effective for H_2S and other reactive thiols, and have been used for intracellular imaging and detection of a variety of reactive thiolates.[4] However, selective discrimination between different biothiols such as glutathione (**GSH**), cysteine (**Cys**) and homocysteine (**Hcy**) remains challenging, because these compounds show similar reactivity patterns from their structurally similar thiol groups. Some reactivity probes for these thiols are known,[5] as well as nanoparticle[6] and MOF-based sensors.[7] Sensors that can discriminate the thiols with high structure similarity, like **Cys**/**Hcy**, or with comparable oxidation potential, like **GSH** vs. **Cys**/**Hcy**, are still needed, however. Another strategy is to use the innate sensitivity of thiols for first row transition metals in the sensing. **GSH**, **Cys** and **Hcy** show strong affinity for Cu^{2+} ions in aqueous solution,[8] and this effect has been coupled with fluorophores for thiol detection, but these studies can be limited in their selectivity.[9]

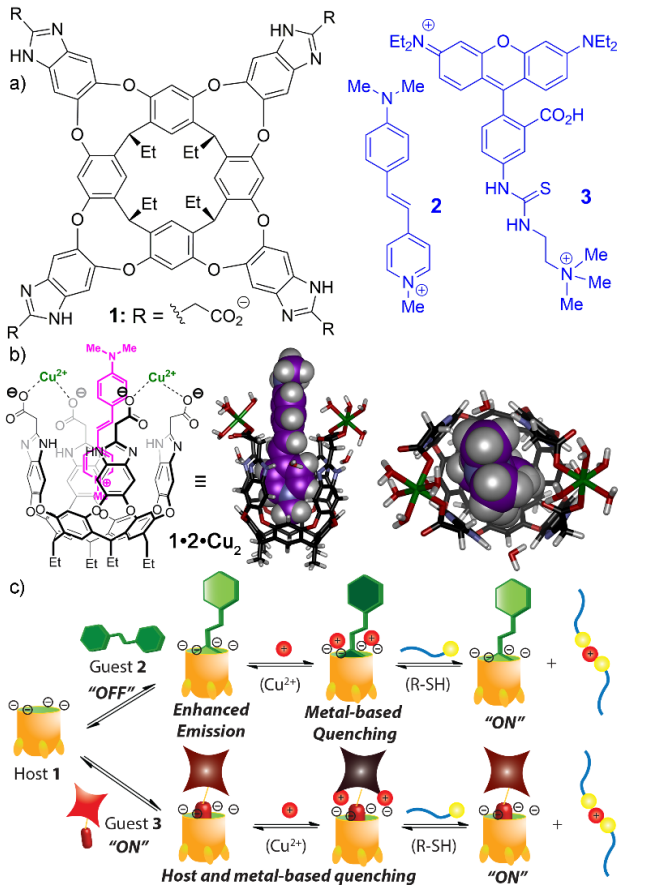

Figure 1. a) Structure of host **1**, guests **2** and **3**; b) minimized structures of **1•2•Cu$_2$** (SPARTAN, semi-empirical minimization); c) Illustration of the turn-on and turn-off fluorescence detection processes for the different fluorophores **2** and **3**.

We hypothesized that non-covalent assembly of the metal ion, fluorophore and a modulator of recognition affinity would allow simple component variation and array-based sensing. This requires that the affinity of all the components for each other

[a]*Department of Chemistry;* [b]*Environmental Toxicology Program;* [c]*Department of Biochemistry and Molecular Biology; University of California-Riverside, Riverside, CA 92521, U.S.A.*
** E-mail: richard.hooley@ucr.edu; wenwan.zhong@ucr.edu*
Electronic Supplementary Information (ESI) available: Experimental details, a table and additional Fig. S1–S8. See DOI: 10.1039/x0xx00000x

must be strong. Recently, we have shown that deep cavitand hosts such as **1** (Figure 1a), when combined with suitable fluorescent guest molecules, can be applied for optical sensing of a variety of structurally similar targets, including modified peptides and small molecules.[10] By combining variably functionalized hosts with different fluorescent guests like **2** and **3** at varying pH in an arrayed format, a "chemical nose" sensor[11] can be created that is capable of highly selective discrimination. Fluorescent guests such as DSMI **2** and Rhodamine B-based guest **3** show variable effects on emission when bound to host **1**. DSMI **2** is a weakly fluorescent dye that is turned-on by binding in the host,[12] whereas guest **3** is strongly quenched upon binding. These responses are modulated upon addition of metal ions to the system: the multiple carboxylate groups in **1** are in close proximity to each other, and are easily capable of free rotation to chelate a metal ion (Figure 1b).[12] Micromolar affinities are possible, even in aqueous solution (K_d (**1•2•Cu²⁺**) = 8.7 μM).[12] Since thiols also show strong affinity for metal ions like Cu and Ni, the metal-containing cavitand sensors could offer an alternative strategy for sensing and discrimination of biothiols (Figure 1c). Here, we show that instead of applying optical sensors that only use "single-mode" detection, one can exploit an arrayed series of host:fluorophore complexes that can discriminate small amounts of biothiols in aqueous solution.

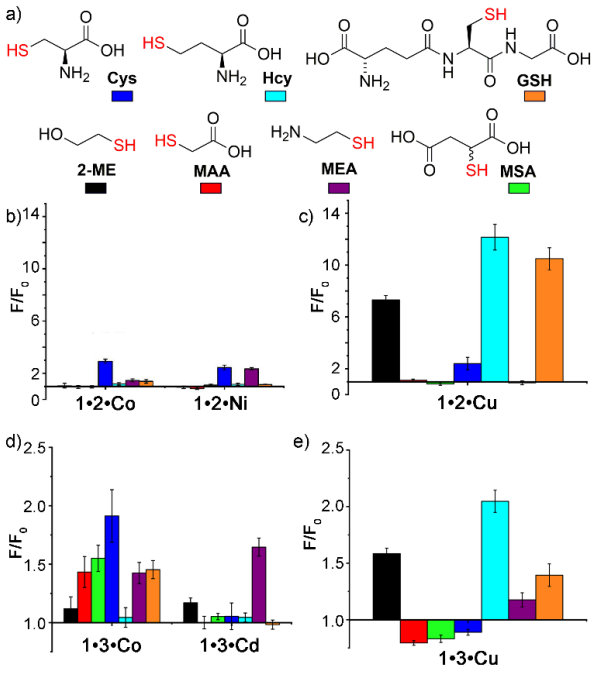

Figure 2. (a) Thiols tested, and fluorescence response of (b) **1•2•Co²⁺, 1•2•Ni²⁺,** (c) **1•2•Cu²⁺;** (d) **1•3•Co²⁺, 1•3•Cd²⁺,** (e) **1•3•Cd²⁺** upon adding different biothiols. Sensor **1•2**: [**1**] = 20 μM, [**2**] = 1.5 μM, [metal] = 10 μM; Sensor **1•3**: [**1**] = 4 μM, [**3**] = 3 μM, [metal] = 10 μM; [RSH] = 100 μM for all. F_0 = fluorescence of the **1•2•M²⁺** or **1•3•M²⁺** complex, respectively.

The seven thiols tested are shown in Figure 2a. These targets included the three most predominant LMW thiols found in cells – **Cys**, **Hcy**, and **GSH**. Other structurally similar, yet non-biological thiols **MAA**, **MEA**, **MSA**, and **2-ME** were included to illustrate the selectivity of the system. The initial tests were performed to determine which transition metals were most effective when combined with host **1** and the two orthogonal fluorophores **2** and **3**. Initially, nine transition metals were tested, forming an array with 18 sensor elements (see Figure S1 for full screen). The thiols ([RSH] = 100 μM) were mixed with the **1•2** or **1•3** sensors and the different metal ions at the optimized host:guest ratios[10b, 12] to ensure maximum signal response (**1•2**:[12] [**1**] = 20 μM, [**2**] = 1.5 μM, **1•3**:[10b] [**1**] = 4 μM, [**3**] = 3 μM, [M] = 10 μM in both cases[12]), and the change in fluorescence (F/F_0) was recorded. The tests were performed in Tris buffer, pH 7.4 to allow mechanistic analysis of the metal effects without other metal cations present (e.g. Na^+ in phosphate buffer). This was only to ensure accuracy, however, Na^+ does not interfere in the response.[12] For **1•2**, only Co^{2+}, Ni^{2+} and Cu^{2+} caused significant changes to at least one biothiol (Figure 2b-c), and Cu^{2+} was by far the most effective additive, with up to a 13-fold enhancement in emission of the **1•2** complex observed with **Hcy**. Most importantly, **Cys** gave only a 2-fold enhancement in signal. The turn-on sensor **1•3** behaved differently, and was variably affected by more metal ions. All thiols tested enhanced the fluorescence for the sensors, with Co^{2+}, Cu^{2+}, Cd^{2+}, and Hg^{2+} showing F/F_0 larger than 50%. Among them, Co^{2+}, Cu^{2+} and Cd^{2+} showed distinct responses to different thiol compounds (Figure 2d, e), but the overall change in fluorescence was smaller than that of **1•2•M²⁺.** Cu^{2+} was still the most responsive added metal. In the absence of metal ions, the influence of biothiols on the host-guest fluorescence was negligible (Figure S-2).

Having narrowed down the most suitable elements for the array, we applied discriminant analysis to determine the most effective sensor for the 7 biothiols tested. We conducted Principal Component Analysis (PCA) on the fluorescence profiles from the sensors (Figure 3 and Figure S-1). We can see from the scores plots of the first two principal components, PC1 and PC2, that the **1•2/1•3** sensors alone are not effective at differentiating the thiols (Figure 3a). Simply adding Cu^{2+} ions to form a 2-component array dramatically improved the separation in the scores plot, clearly illustrating the importance of Cu^{2+} in thiol recognition (Figure 3b). 95% confidence ellipses on the scores plot shows good clustering of the repeated measurements of the same compound. Importantly, **Cys**, **Hcy**, and **GSH** were well separated even with this minimal array, but **Cys** could not be differentiated from **MSA** and **MAA**, and separation between **GSH** and **2-ME** was poor. To further improve the separation, we formed a 4-component array by adding multiple metal ions to **1•2**, while retaining only **1•3•Cu²⁺** (Figure 3c), and a 6-component array including three metal ions for each sensor (Figure 3d). The 4-component array was the optimal sensor combination, combining a minimal number of components with almost complete target discrimination (although differentiating **MAA** and **MSA** remained problematic). The six-component array was most effective, but not significantly so. Further analysis of the loading data (Table S-1) from PCA shows that **1•3•Cd²⁺** and **1•3•Co²⁺** contribute poorly to differentiation of these compounds, as so the optimal array was determined to be **1•2•Co²⁺**, **1•2•Ni²⁺**, **1•2•Cu²⁺** and **1•3•Cu²⁺** (Figure 3c). The separation effect using this 4-sensor array was also verified by hierarchical cluster analysis (HCA) (Figure S-3). This illustrates that **Cys**, **MEA**, **Hcy**, and **GSH** can be

well separated with comparable dissimilarity degrees. These four thiols have a larger dissimilarity with **2-ME**, **MSA** and **MAA**, with the latter two not differentiable from each other.

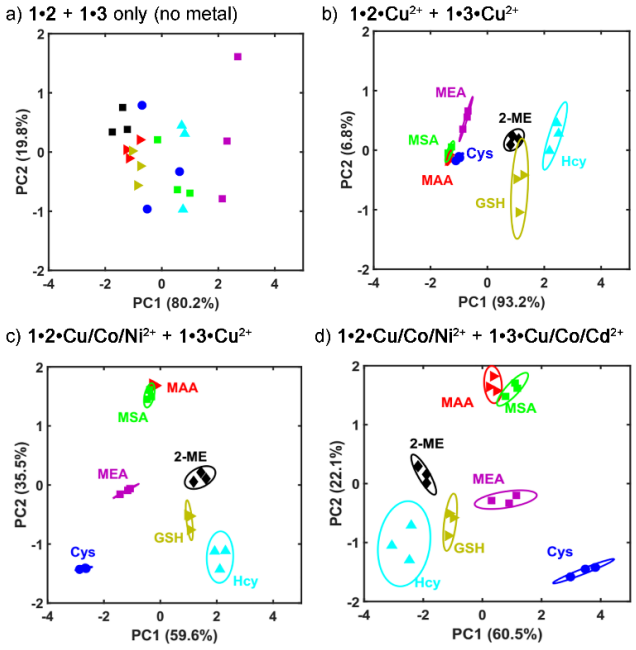

Figure 3. PCA scores plots showing the effect of biothiol differentiation using a) the no-metal cavitand sensors **1•2** and **1•3**; b) the Cu-containing cavitand sensors **1•2•Cu²⁺** and **1•3•Cu²⁺**; c) a total of four sensors: **1•2•Co²⁺**, **1•2•Ni²⁺** and the two Cu-containing cavitand sensors; and d) all six sensors showing the largest fluorescence changes in Figure 2, i.e. **1•2•Co²⁺**, **1•2•Ni²⁺**, **1•2•Cu²⁺**, **1•3•Co²⁺**, **1•3•Cu²⁺** and **1•3•Cd²⁺**. The sensor concentrations were the same as in Figure 2.

The mechanism of the sensing process is illustrated in Figure 1c. Small water-soluble molecules are not bound in **1**, nor are they competitive guests when compared to the affinity of **2** or **3**. Instead, the strong affinity of the biothiols for ions such as Co/Cu or Ni competes with the **1•2** and **1•3** complexes for the metal ions (e.g. log K_1 (Cu(II)•GSH) = 8.06[13a], log K_1 (Cu(II)•Cys) = 9.3[13b]). The metals modulate the emission of **1•2** and **1•3**, mainly via heavy atom quenching effects, but also *via* guest displacement.[12] The thiols sequester the metal ions, causing selective changes in fluorescence of **1•2** and **1•3**. The varying affinities of the different biothiols for the different metals, coupled with the varying affinities of the different metals for **1•2** and **1•3** causes the differential responses. As Cu^{2+} has the strongest affinity for thiols, this shows the greatest amount of metal sequestration, thus the strongest signal. This is corroborated by the fact that only thiols caused a response, not disulfides. Indeed, cystine (the disulfide of **Cys**) had no impact on the fluorescence of **1•2•Co²⁺** with a concentration as high as 200 μM, while the signal of **Cys** increased with **Cys** concentration (Figure S-8). In addition, SELDI-MS analysis showed that the proportion of **1•Cu²⁺** in solution decreased markedly (and variably) in the presence of different thiols (Figures S-4, S-5).

The most intriguing result is the differentiation of **Cys** and **Hcy** with our sensors. Selective detection of **Hcy** is more challenging than detection of **Cys**, and only a few such probes have been reported.[5d,5h,5i,7,14] The large separation between these two compounds on the PCA scores plot and on the HCA chart is due to their differential responses with the multiple sensor elements in the array. For example, upon increasing thiol concentration from 0 – 1,000 μM, **1•2•Co²⁺** and **1•2•Ni²⁺** responded to only **Cys** but not **Hcy**, whereas **Hcy** increases the fluorescence of **1•2•Cu²⁺** and **1•3•Cu²⁺**, but **Cys** does not (Figures S-6, S-7). As such, the 3-component **1•2•Co²⁺/Ni²⁺/Cu²⁺** array was applied to detect variations in the relative ratio of **Cys/Hcy**. The proportion of **Hcy** in the mixture was varied from 0 to 100%, keeping the total concentration of both thiols at 100 μM. As shown in Figure 4, decreasing the proportion of **Cys** in the **Cys-Hcy** mixture did not affect the no-metal control (**1•2** only), but caused substantial signal decrease with the **1•2•Co²⁺** sensor, and a mild decrease with **1•2•Ni²⁺**. In contrast, a high proportion of **Cys** did not generate much fluorescence change in **1•2•Cu²⁺**, and significant signal increase was observed with the proportion of **Hcy** higher than 50%. To visualize the change better, PCA was performed using the 3-component array, and this shows that the **Cys/Hcy** ratio increases along with the increase of PC1. The value of PC2 initially decreased with the proportion of **Cys** in the mixture, and then increased with higher proportion of **Hcy** which agrees with the opposite trend of signal change between **1•2•Co²⁺** and **1•2•Cu²⁺**.

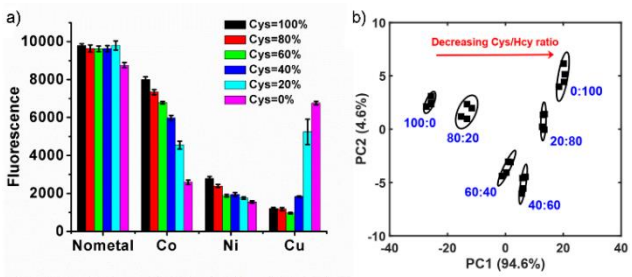

Figure 4. Quantifying the binary mixture of **Cys**/**Hcy** with the ratio of these two changing from 0:100% to 100%:0 in 20% increments. [**Hcy**+**Cys**] = 100 μM. a) Fluorescence signals and b) PCA scores plot obtained with the three sensors **1•2•Co²⁺**, **1•2•Ni²⁺** and **1•2•Cu²⁺**.

Varying the components allows selectivity for different thiols. Whereas **1•2•Cu²⁺** sensor shows the greatest response for **Hcy** and **GSH**, only **Cys** induced a large fluorescence change (F/F_0 ~ 3 in Figure 2) with the **1•2•Co²⁺** sensor. The detection performance for this sensor for **Cys** was then tested within a concentration range of 0 – 200 μM (Figure S-8). Continuous fluorescence increase with increasing **Cys** concentration was observed until plateauing at 200 μM, and the calculated limit of detection (LOD) was 3.19 μM (Figure S-9). This LOD is sufficient for detection of **Cys** in biological samples, as the free **Cys** in human plasma is ~8-10 μM.[2f] The detection performance for other thiols was also determined. The **1•2•Ni²⁺** sensor responded to both **Cys** and **MEA** (Figure S-10), and the LOD for **Cys** was 4.32 μM, comparable to that of **1•2•Co²⁺**, but the dynamic range of this sensor was larger: fluorescence continued to increase until the thiol concentration reached 1 mM. The **1•2•Cu²⁺** sensor exhibited strong response to **Hcy**, to 2.02 μM, and **GSH**, to 2.87 μM (Figure S-10), but low response to **Cys**.

We further evaluated whether our sensors could detect these thiols in a complex biorelevant environment. Each thiol compound was added to the lysate of MCF-7 breast cancer cells prepared from ~10^6 cells/mL, and then the **1•2•Cu^{2+}** sensor was added. The resultant fluorescence signal was fit to the calibration curve of the corresponding thiol standard to calculate the thiol concentration. The calculated concentration was divided by the spiked thiol concentration to result in the recovery values shown in Table 1. To better assess the accuracy of our method, we subtracted the background fluorescence before recovery calculation, which may come from endogenous thiols in the sample. We can see that the calculated value matches quite well with the spiked-in concentration, illustrating that the sensor is tolerant to cell lysate background, retaining the ability to provide accurate measurement of the LMW thiols.

Table 1. Detection of spiked **Cys**, **Hcy** and **GSH** in MCF-7 cell lysate using the **1•2•Cu^{2+}** sensor.[a]

Biothiol	Spiked (μM)	Tested (μM)	Recovery
Cys	100	108.3	108.3%
Hcy	50	53.2	106.5%
GSH	100	107.1	107.1%

[a] [**Cys**],[**GSH**] = 100 μM, [**Hcy**] = 50 μM.

In conclusion, we have shown that a synergistic combination of a deep cavitand host, fluorophore guests and transition metal ions can be used to sense small molecule thiols of biological interest. Excellent selectivity between the three most common LMW biothiols is possible, as well as successful discrimination from other small thiols with similar structures. Thiol-metal coordination and host-fluorophore interactions both contribute to the signal variation induced by different biothiols, maximizing the selectivity of the detection. The sensors are functional in aqueous solution and even in cell extracts. This flexible, yet simple sensor array represents a valuable tool for monitoring the presence of biologically important thiols in complex media.

The authors would like to thank the National Science Foundation (CHE-1707347) for support.

Conflicts of interest

There are no conflicts to declare.

Notes and references

1 a) H. Refsum, A. D. Smith, P. M. Ueland, E. Nexo, R. Clarke, J. McPartlin, C. Johnston, F. Engbaek, J. Schneede, C. McPartlin and J. M. Scott, *Clin. Chem.*, 2004, **50**, 3; b) L. B. Poole, *Free Radic. Biol. Med.*, 2015, **80**, 148.

2 a) L. Turell, D. A. Vitturi, E. L. Coitino, L. Lebrato, M. N. Moller, C. Sagasti, S. R. Salvatore, S. R. Woodcock, B. Alvarez and F. J. Schopfer, *J. Biol. Chem.*, 2017, **292**, 1145; b) J. L. Luebke and D. P. Giedroc, *Biochemistry*, 2015, **54**, 3235; c) M. L. Reniere, A. T. Whiteley, K. L. Hamilton, S. M. John, P. Lauer, R. G. Brennan and D. A. Portnoy, *Nature*, 2015, **517**, 170; d) J. Wong, Y. Chen and Y.-H. Gan, *Cell Host Microbe*, 2015, **18**, 38; e) Z. A. Stapper and T. R. Jahn, *Cell Rep.*, 2018, **24**, 1696; f) Van Laer, K.; Hamilton, C. J.; Messens, J., *Antioxid. Redox Signal.* 2013, **18**, 1642.

3 a) S. T. Manjare, Y. Kim and D. G. Churchill, *Acc. Chem. Res.*, 2014, **47**, 2985; b) L.-Y. Niu, Y.-Z. Chen, H.-R. Zheng, L.-Z. Wu, C.-H. Tung and Q.-Z. Yang, *Chem. Soc. Rev.*, 2015, **44**, 6143; c) C.-X. Yin, K.-M. Xiong, F.-J. Huo, J. C. Salamanca and R. M. Strongin, *Angew. Chem. Int. Ed.*, 2017, **56**, 13188; d) V. S. Lin, W. Chen, M. Xian and C. J. Chang, *Chem. Soc. Rev.*, 2015, **44**, 4596.

4 a) A. R. Lippert, E. J. New and C. J. Chang, *J. Am. Chem. Soc.*, 2011, **133**, 10078; b) T. S. Bailey and M. D. Pluth, *J. Am. Chem. Soc.*, 2013, **135**, 16697; c) V. S. Lin, A. R. Lippert and C. J. Chang, *Proc. Natl. Acad. Sci. U. S. A.*, 2013, **110**, 7131.

5 a) W. Wang, O. Rusin, X. Xu, K. K. Kim, J. O. Escobedo, S. O. Fakayode, K. A. Fletcher, M. Lowry, C. M. Schowalter, C. M. Lawrence, F. R. Fronczek, I. M. Warner and R. M. Strongin, *J. Am. Chem. Soc.*, 2005, **127**, 15949; b) N. Shao, J. Y. Jin, S. M. Cheung, R. H. Yang, W. H. Chan and T. Mo, *Angew. Chem. Int. Ed.*, 2006, **45**, 4944; c) S. V. Mulay, Y. Kim, M. Choi, D. Y. Lee, J. Choi, Y. Lee, S. Jon and D. G. Churchill, *Anal. Chem.*, 2018, **90**, 2648; d) X. Yang, Y. Guo and R. M. Strongin, *Angew. Chem. Int. Ed.*, 2011, **50**, 10690; e) L.-Y. Niu, Y.-S. Guan, Y.-Z. Chen, L.-Z. Wu, C.-H. Tung and Q.-Z. Yang, *J. Am. Chem. Soc.*, 2012, **134**, 18928; f) M. D. Hammers and M. D. Pluth, *Anal. Chem.*, 2014, **86**, 7135; g) F. Wang, L. Zhou, C. Zhao, R. Wang, Q. Fei, S. Luo, Z. Guo, H. Tian and W.-H. Zhu, *Chem. Sci.*, 2015, **6**, 2584; h) M.-Y. Jia, L.-Y. Niu, Y. Zhang, Q.-Z. Yang, C.-H. Tung, Y.-F. Guan and L. Feng, *ACS Appl. Mater. Interfaces*, 2015, **7**, 5907; i) Z.-H. Fu, X. Han, Y. Shao, J. Fang, Z.-H. Zhang, Y.-W. Wang and Y. Peng, *Anal. Chem.*, 2017, **89**, 1937.

6 a) J. Deng, Q. Lu, Y. Hou, M. Liu, H. Li, Y. Zhang and S. Yao, *Anal. Chem.*, 2015, **87**, 2195; b) L. Zhang, Z. Wang, J. Hou, L. Lei, J. Li, J. Bai, H. Huang and Y. Li, *Anal. Methods*, 2018, **10**, 2560.

7 J. Wang, Y. Liu, M. Jiang, Y. Li, L. Xia and P. Wu, *Chem. Commun.*, 2018, **54**, 1004.

8 V.G. Shtyrlin, Y.I. Zyavkina, V.S. Ilakin, A.V. Zakharov, *J. Inorg. Biochem.* 2005, **99**, 1335.

9 a) Z. Liu, W. He and Z. Guo, *Chem. Soc. Rev.*, 2013, **42**, 1568; b) J. Sun, F. Yang, D. Zhao, C. Chen and X. Yang, *ACS Appl. Mater. Interfaces*, 2015, **7**, 6860; c) Y. Hu, C. H. Heo, G. Kim, E. J. Jun, J. Yin, H. M. Kim and J. Yoon, *Anal. Chem.*, 2015, **87**, 3308; d) Y. L. Duan, Y. G. Shi, J. H. Chen, X. H. Wu, G. K. Wang, Y. Zhou and J. F. Zhang, *Tetrahedron Lett.*, 2012, **53**, 6544; e) H. Wang, G. Zhou and X. Chen, *Sens. Actuators, B,* 2013, **176**, 698; f) Loas, A.; Radford, R. J.; Deliz Liang, A.; Lippard, S. J., *Chem. Sci.* **2015**, *6*, 4131; g) H. Xu and M. Hepel, *Anal. Chem.*, 2011, **83**, 813.

10 a) Y. Liu, L. Perez, M. Mettry, C. J. Easley, R. J. Hooley and W. Zhong, *J. Am. Chem. Soc.*, 2016, **138**, 10746; b) Y. Liu, L. Perez, M. Mettry, A. D. Gill, S. R. Byers, C. J. Easley, C. J. Bardeen, W. Zhong and R. J. Hooley, *Chem. Sci.*, 2017, **8**, 3960.

11 H. S. Hewage and E. V. Anslyn, *J. Am. Chem. Soc.*, 2009, **131**, 13099.

12 Y. Liu, M. Mettry, A. D. Gill, L. Perez, W. Zhong and R. J. Hooley, *Anal. Chem.*, 2017, **89**, 11113.

13 a) P.K. Singh, B.S. Garg, D. N. Kumar, B.K. Singh, *Ind. J. Chem.* 2001, **40**, 1339; b) G.R. Lenz, A.E. Martell, *Biochemistry,* 1964, **3**, 745.

14 H. Li, J. Fan, J. Wang, M. Tian, J. Du, S. Sun, P. Sun and X. Peng, *Chem. Commun.,* **2009**, 5904.

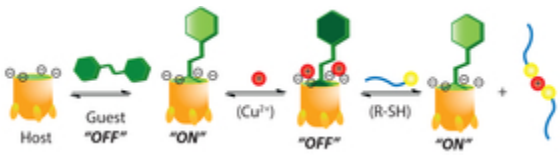

23x6mm (300 x 300 DPI)